

Estimating and detecting random processes on the unit circle

Changrong Liu* S. Suvorova** R. J. Evans** W. Moran**
A. Melatos***

* *Electrical and Electronic Engineering Department, University of Melbourne, Parkville, Victoria 3010, Australia and OzGrav (e-mail: changrongl1@student.unimelb.edu.au)*

** *Electrical and Electronic Engineering Department, University of Melbourne, Parkville, Victoria 3010, Australia and OzGrav (e-mail: sofia.suvorova, robinje, wmoran@unimelb.edu.au).*

*** *School of Physics, University of Melbourne, Parkville, Victoria 3010, Australia and OzGrav (e-mail: amelatos@unimelb.edu.au).*

Abstract: Detecting random processes on a circle has been studied for many decades. The Neyman-Pearson detector, which evaluates the likelihood ratio, requires first the conditional mean estimate of the circle-valued signal given noisy measurements, which is then correlated with the measurements for detection. This is the estimator-correlator detector. However, generating the conditional mean estimate of the signal is very rarely solvable. In this paper, we propose an approximate estimator-correlator detector by estimating the truncated moments of the signal, with estimated signal substituted into the likelihood ratio. Instead of estimating the random phase, we estimate the complex circle-valued signal directly. The effectiveness of the proposed method in terms of estimation and detection is shown through numerical experiments, where the tracking accuracy and receiver operating curves, compared with the extended Kalman filter are shown under various process/measurement noise.

Keywords: Conditional Mean Estimate, Circle-Valued Signal, Estimator-Correlator, Moment Function, Random Process

1. INTRODUCTION

Detecting weak circle-valued random processes in white Gaussian noise has been analyzed by researchers for several decades. This type of signal is widely encountered in a range of fields including communication systems, where signals are modelled as either frequency or phase modulated by a Gaussian message (Snyder (1968)). Another example is optical communication with laser phase drift (Rusch and Poor (1995); Foschini et al. (1988)). Generally speaking, These signals are specific cases of non-Gaussian random processes (Kailath and Poor (1998)). In order to construct a Neyman-Pearson detector for such a process, the likelihood ratio must be evaluated, which requires computation of the causal conditional mean estimate of the random process given measurements. The estimated signal is then correlated with the measurements to produce the detection statistic (Kailath and Poor (1998); Veeravalli and Poor (1991)). This is the estimator-correlator (EC) detector (Kailath and Poor (1998)). Unfortunately, the conditional mean estimate is mostly impossible to compute except in the Gaussian case (Kailath and Poor (1998)). Instead, a near-optimal approximation of the conditional mean estimate (or equivalently, the conditional density) of the signal has to be constructed.

For circle-valued signals, various approximation techniques have been proposed. A random point on the circle is

represented either by the angle $\Theta \in [-\pi, \pi)$ or the complex numbers $\{e^{i\Theta} | \Theta \in [-\pi, \pi)\}$. One approach is to characterize the conditional density of Θ using a Gaussian sum approximation with the mean and variance updated, as described in Tam and Moore (1977). In Willsky (1974), the density of Θ is spanned by Fourier modes, with Fourier coefficients estimated. In Suvorova et al. (2021), the density of Θ is approximated by a von-Mises distribution with maximum entropy, and at each iteration, the density is propagated and projected back to a von-Mises distribution. Another approach is to use the extended Kalman filter (EKF) to linearize the nonlinear system dynamics and/or the measurement process to demodulate (estimate) the phase (Georghiadis and Snyder (1985); Snyder (1968)). In Tretter (1985), the unwrapped phase model is assumed and fitted by a linear regression. In Scharf et al. (1980), the dynamics of the wrapped phase sequence is assumed and then estimated using dynamic programming. A similar idea has also been proposed in Suvorova et al. (2018) and Melatos et al. (2021), where the phase is modelled as a hidden Markov model and the Viterbi algorithm is used to track the random phase. A deterministic filtering approach is attempted in Zamani et al. (2011), where the process and measurement noises are both treated as unknown deterministic disturbances and a deterministic minimum-energy filter is formed by minimizing an energy cost function over phase trajectories (Coote et al. (2009)). As we can see, a large number of

methods have been considered for estimating (filtering) the phase Θ , while very few papers analyze the complex signal $e^{i\Theta}$ directly. One recent paper (Condat (2021)) minimizes a Tikonov-regularized problem over the complex signal $e^{i\Theta}$, where the non-convexity introduced by the S^1 constraint is relaxed using moments of measures.

In this paper, we focus directly on stochastic filtering of the circle-valued signal $e^{i\Theta}$ embedded in large additive white noise, where Θ obeys different random processes. We first present the nonlinear Kushner stochastic partial differential equation for recursively computing the conditional mean estimate of the signal, or equivalently, the conditional probability density. The solution of this equation is infinite dimensional, and we approximate it by a sequence of moment functions. The choice of moment functions is determined by the fact that they form the eigenspace of the infinitesimal generator of the signal process. In doing so, solving the Kushner equation simplifies to solving a sequence of time-dependent ordinary differential equations (ODEs), which characterize the evolution of the conditional density. We then produce the approximate optimal EC detector and show its performance by simulations.

The paper is organized as follows. Section 2 describes the dynamic system on S^1 and formulates the detection and estimation problems. The Kushner equation for computing the conditional density and its finite-dimensional approximation is introduced and derived in Section 3. Simulation results are included in Section 4, testing both estimation and detection performance, compared with EKF based methods. Finally, brief conclusions are drawn in Section 5.

2. PROBLEM FORMULATION

2.1 System model

Consider a detection system with two hypothesis:

$$H_0 : Z_t = \sigma_0^{1/2} W_t, \quad 0 \leq t \leq T, \quad (1)$$

$$H_1 : Z_t = \int_0^t h(X_s) ds + \sigma_0^{1/2} W_t, \quad 0 \leq t \leq T \quad (2)$$

where Z_t is the noisy measurements and $X_t = e^{i\Theta_t} \in S^1$ is the circle-valued signal with Θ_t obeying an arbitrary random process. Measurement function $h(X_t)$ in our case, is given by

$$h(X_t) = \Re[X_t] \quad (3)$$

with $\Re[\cdot]$ denoting the real part. $\{W_t, 0 \leq t \leq T\}$ is the standard Wiener process, which represents the measurement noise and is independent of X_t . σ_0 denotes the variance of the measurement noise and is assumed known. In this paper, we consider three specific random processes for Θ_t :

$$(i) \quad \Theta_t = \int_0^t q_\Theta^{1/2} dB_s + \phi_0, \quad (4)$$

$$(ii) \quad \Theta_t = \int_0^t (w_0 ds + q_\Theta^{1/2} dB_s) + \phi_0, \quad \text{and} \quad (5)$$

$$(iii) \quad \Theta_t = \int_0^t (w_s ds + q_\Theta^{1/2} dB_s) + \phi_0, \quad (6)$$

$$w_t = w_0 + \int_0^t q_w^{1/2} d\tilde{B}_s$$

where q_Θ and q_w are known functions of phase, Θ , and frequency, w . They represent the noise variance for phase and frequency, respectively. w_0 is the known initial frequency and ϕ_0 is the random initial phase, uniformly distributed across $[0, 2\pi)$. $\{B_t, 0 \leq t \leq T\}$ and $\{\tilde{B}_t, 0 \leq t \leq T\}$ are two independent standard Wiener processes, which are also independent of X_t and $\{W_t, 0 \leq t \leq T\}$.

2.2 Neyman-Pearson detector

The Neyman-Pearson (EC) detector is the optimal detector in the sense that it maximizes the detection probability (Pd) with given false alarm probability (Pf). In order to form this type of detector, the log likelihood ratio $\log \Lambda_t$ has to be evaluated, which is given by

$$\log \Lambda_t = \int_0^t \hat{X}_s dZ_s - \frac{1}{2} \int_0^t \hat{X}_s^2 ds, \quad (7)$$

$$\hat{X}_t = \mathbf{E}[X_t | \mathcal{F}_t; H_1] \quad (8)$$

with \mathcal{F}_t the filtration of σ -algebras generated by $\{Z_\tau, 0 \leq \tau \leq t\}$, given in (2) with $\mathcal{F}_s \subseteq \mathcal{F}_t, \forall s \leq t$.

From (7) and (8), the EC detector is formed in two steps: 1.) calculate the conditional mean estimate \hat{X}_t ; 2.) form the log likelihood ratio $\log \Lambda_T$ at the termination time T and compare it with a pre-specified threshold to claim H_0 or H_1 correspondingly.

3. NONLINEAR FILTERING: COMPUTE CONDITIONAL MEAN ESTIMATE

We now consider computation of the conditional mean estimate of the signal using the Kushner equation.

3.1 Kushner equation: recursive filtering of the conditional density

Given the filtered probability space $(\Omega, \mathcal{F}, \mathbb{P}; \{\mathcal{F}_t\})$ with Ω the underlying sample space and \mathbb{P} the probability measure defined on \mathcal{F} , suppose the signal and measurement processes are given by

$$\begin{aligned} dx_t &= b(x_t)dt + \sigma(x_t)dB_t, \quad x(0) = x_0 \\ dZ_t &= h(x_t)dt + \sigma_0^{1/2}dW_t, \quad Z_0 = 0 \end{aligned} \quad (9)$$

with $x_t \in \mathbb{R}^d$ and $b : \mathbb{R}^d \rightarrow \mathbb{R}^d, \sigma : \mathbb{R}^d \rightarrow \mathbb{R}^{d \times p}, h : \mathbb{R}^d \rightarrow \mathbb{R}, a \triangleq \frac{1}{2}\sigma\sigma^T$ with superscript T being the transpose of a matrix. The filtering problem can be formulated as: for a general measurable function $g(x_t)$, calculate $\hat{g}(x_t)$ by

$$\begin{aligned} \hat{g}(x_t) &\triangleq \mathbf{E}[g(x_t) | \mathcal{F}_t] \\ &= \int_{\mathbb{R}^d} g(x_t) \mathbb{P}(x_t \in dx | \mathcal{F}_t) \\ &= \int_{\mathbb{R}^d} g(x) p(x, t | \mathcal{F}_t) dx \end{aligned} \quad (10)$$

where $p(x, t | \mathcal{F}_t)$ denotes the conditional density of x at time t . The recursive formula for evolving $p(x, t | \mathcal{F}_t)$ is described by the Kushner equation (Kushner (1967))

$$\begin{aligned} dp(x, t | \mathcal{F}_t) &= \mathcal{L}^* p(x, t | \mathcal{F}_t) dt \\ &\quad + (h(x_t) - \hat{h}(x_t)) \cdot \sigma_0^{-1} [dZ_t - \hat{h}(x_t)dt] p(x, t | \mathcal{F}_t) \end{aligned} \quad (11)$$

with \mathcal{L}^* the adjoint of the infinitesimal generator \mathcal{L} , given respectively by

$$\mathcal{L}^*(\cdot) = \sum_{i,j=1}^d \frac{\partial^2}{\partial x_i \partial x_j} (a_{ij}(\cdot)) - \sum_{i=1}^d \frac{\partial}{\partial x_i} (b_i(\cdot)), \quad (12)$$

$$\mathcal{L}(\cdot) = \sum_{i,j=1}^d a_{ij} \frac{\partial^2}{\partial x_i \partial x_j} + \sum_{i=1}^d b_i \frac{\partial}{\partial x_i}. \quad (13)$$

To uniquely characterize the conditional density, we pair (11) with an arbitrary test function $g(x)$ with compact support, where the duality pairing is denoted by $\langle \cdot, \cdot \rangle$. We then have

$$\begin{aligned} d\langle p(x, t|\mathcal{F}_t), g(x) \rangle &= \langle \mathcal{L}^* p(t, x|\mathcal{F}_t), g(x) \rangle dt + \langle (h - \hat{h}) \\ &\quad \cdot \sigma_0^{-1} [dZ_t - \hat{h} dt] p(x, t|\mathcal{F}_t), g(x) \rangle \end{aligned} \quad (14)$$

which further implies

$$\begin{aligned} d\hat{g}(x_t) &= \mathcal{L}\hat{g}(x_t) dt \\ &\quad + \langle g(x_t)h(x_t) \rangle - \hat{g}(x_t)\hat{h}(x_t) \cdot \sigma_0^{-1} [dZ_t - \hat{h}(x_t)dt], \end{aligned} \quad (15)$$

here \mathcal{L} is defined in (13). Both $\hat{\cdot}$ and $\langle \cdot \rangle$ denote the conditional mean with respect to the conditional density $p(x, t|\mathcal{F}_t)$. $\hat{g}(x_t) \triangleq \langle p(x, t|\mathcal{F}_t), g(x) \rangle$ is defined in (10).

3.2 Choice of the test function

From the previous section, we observe the duality relationship between the conditional density and the estimated test function. In order to fully characterize $p(x, t|\mathcal{F}_t)$, an infinite number of statistics (or test functions $g(\cdot)$) are required. In this paper, we set the test functions to be the moment functions of the signal X_t , given as $X_n(t) \triangleq e^{in\Theta t}$ for $n = 0, \dots, N-1$, considering firstly, $X_n(t)$ can be regarded as the characteristic function of Θ , which completely determines the properties of the probability distribution of Θ . Secondly, $X_n(t)$ spans the eigenspace of the generator \mathcal{L} , as discussed in the following section. In doing so, solving an infinite dimensional Kushner equation boils down to solving N 's ODEs.

As we can see from (15), the filtering process is composed of two terms: the one-step prediction (the first term) and the update (the second term). We will derive the solutions for \hat{X}_n in terms of these two properties.

3.3 Prediction: compute $\mathcal{L}\hat{X}_n(t)$

In order to obtain the infinitesimal generator of the signal process, we need to write the signal dynamics in Ito differential form, for three scenarios. In particular, we have for scenario (i) and (ii)

$$(i) \quad dX_n = -\frac{q\Theta n^2}{2} X_n dt + inq_{\Theta}^{1/2} X_n dB_t, \quad (16)$$

$$(ii) \quad dX_n = (inw_0 - \frac{q\Theta n^2}{2}) X_n dt + inq_{\Theta}^{1/2} X_n dB_t. \quad (17)$$

Comparing (17) with (16), a constant rotation term inw_0 is added to the drift coefficient. Considering the martingale process in both circumstances: $inq_{\Theta}^{1/2} X_n dB_t$, with

the property $\mathbf{E}[\int_s^t inq_{\Theta}^{1/2} X_n(\tau) dB_{\tau} | \mathcal{F}_s] = 0$, we have a separate infinitesimal generator for each X_n , where $\mathcal{L}_n = inw_0 - \frac{q\Theta n^2}{2}$, with $w_0 = 0$ in scenario (i).

The differential equation for X_n in scenario (iii) can be obtained in the same manner

$$dX_n = (inw_t - \frac{q\Theta n^2}{2}) X_n dt + inq_{\Theta}^{1/2} X_n dB_t. \quad (18)$$

However, as shown here, the randomness appears in the drift coefficient. Now it is difficult to interpret the generator by simply writing $\mathcal{L}_n(w) = inw(t) - \frac{q\Theta n^2}{2}$ with $w(t)$ a random process. Instead, $\mathcal{L}_n(w)$ should be interpreted in the mean sense by marginalizing out the random variable $w(t)$. In other words, we have the infinitesimal generator computed by $\mathcal{L}_n = \mathbf{E}_w[\mathcal{L}_n(w)|\mathcal{F}_t] = \int_{w \in \mathbb{R}} \mathcal{L}_n(w) p(w, t|\mathcal{F}_t) dw$, with $d\hat{X}_n - \mathcal{L}_n \hat{X}_n dt$ still a martingale process. Alternatively, we introduce the new state variables as $X_{mn} \triangleq w^m e^{in\Theta}$, with $m = 0, \dots, M-1$ and $n = 0, \dots, N-1$, where superscript m and n denote the m th and n th power, respectively. This is an "augmented" state space by noting that $X_n = X_{mn}|_{m=0}$. For predicting X_{mn} , likewise, we write down the differential equation for X_{mn} as

$$\begin{aligned} (iii) \quad dX_{mn} &= \left(\frac{q_w m(m-1)}{2} X_{m-2,n} + inX_{m+1,n} \right. \\ &\quad \left. - \frac{q_{\Theta} n^2}{2} X_{mn} \right) dt + q_w^{1/2} m X_{m-1,n} d\tilde{B}_t \\ &\quad + inq_{\Theta}^{1/2} X_{mn} dB_t \end{aligned} \quad (19)$$

with $\mathcal{L}_{mn}(X_{mn}) = \frac{q_w m(m-1)}{2} X_{m-2,n} + inX_{m+1,n} - \frac{q_{\Theta} n^2}{2} X_{mn}$ for each X_{mn} . Here by augmenting the state space from X_n to X_{mn} , the time-variant generator is replaced by a time-invariant generator at the cost of higher computational complexity.

3.4 Update: incorporate the innovation $dZ_t - \hat{h} dt$

In all three scenarios, we have measurement function $h(X_t) = \Re[X_t]$ from (3). This is a considerable advantage since h can be regarded as a linear operator in both the subspace $\{X_n\}_{n=0}^{N-1}$ and $\{X_{mn}\}_{m=0, n=1}^{M-1, N-1}$ by noting

$$\begin{aligned} (i) \&(ii) \quad \langle hX_n \rangle &= \left\langle \frac{X_{n+1} + X_{n-1}}{2} \right\rangle \\ \hat{h} &= \frac{\hat{X}_1 + \hat{X}_1^*}{2}, \end{aligned} \quad (20)$$

$$\begin{aligned} (iii) \quad \langle hX_{mn} \rangle &= \left\langle \frac{X_{m,n+1} + X_{m,n-1}}{2} \right\rangle \\ \hat{h} &= \frac{\hat{X}_{01} + \hat{X}_{01}^*}{2} \end{aligned} \quad (21)$$

with $(\cdot)^*$ denoting the complex conjugation. Combining (16), (17), (19) with (20), (21) and substituting into (15), we can compute $\hat{X}_n(t)$ for (i)&(ii) and $\hat{X}_{mn}(t)$ for (iii) recursively by solving a sequence of stochastic ODEs.

The log-likelihood ratio, defined in (7) can then be updated recursively as well by substituting in \hat{X}_t from (15) without too much effort, considering $\hat{X}_t = \hat{X}_n(t)|_{n=1}$ for (i)&(ii) and $\hat{X}_t = \hat{X}_{mn}(t)|_{m=0, n=1}$ for (iii).

4. SIMULATIONS AND RESULTS

4.1 Implementation of the Neyman-Pearson (EC) detector

Since scenario (i) is analogous to (ii) with $w_0 = 0$, we only do experiments for (ii) and (iii). The Neyman-Pearson (EC) detector is composed of a conditional mean estimator and a log-likelihood ratio detector, hence we need to check the performance of both estimation and detection. For estimation, we generate the synthetic signal $X_{\text{syn}} = A_{\text{syn}} e^{i\Theta_{\text{syn}}}$ with Θ_{syn} given in (5) and (6). Noisy measurements are generated from (2). For detection, we randomly generate measurements from (1) or (2), where signal $X_{\text{syn}} = A_{\text{syn}} e^{i\Theta_{\text{syn}}}$ is generated as above. We fix termination time T and compare $\log \Lambda_T$ with a pre-specified threshold and claim detection if $\log \Lambda_T$ is greater than the threshold, and vice versa. We simulate both the signal process and the measurement process numerically using the Euler-Maruyama method with sampling interval $\Delta t = 0.1$ s. The parameters are listed in Table 1.

Table 1. Simulation parameters

parameter	description	value
ϕ_0	initial phase	$\overset{\text{dist}}{\sim} U(0, 2\pi)$
q_Θ	phase noise variance	$10^{-1}, 10^{-2}$
q_w	frequency noise variance	10^{-8}
σ_0	observation noise variance	$1, \dots, 80$
w_0	initial frequency	0.012, 0.032Hz
$ A_{\text{syn}} $	absolute amplitude of synthetic signal	1
$\text{SNR} = \sqrt{\frac{ A_{\text{syn}} \Delta t}{\sigma_0}}$	signal to noise ratio	0.0354, ... 0.3162
$N - 1$	highest moment of X_t	11
$M - 1$	highest moment of w_t	3
Δt	sampling time interval	10^{-1} sec
L	length of synthetic data	10^4
$T = L\Delta t$	termination time	10^3 sec

4.2 Estimation performance

Two realizations of EC estimated $\Re[\hat{X}_t]$, with phase dynamics described in (ii) and (iii) are shown in Fig. 1 and Fig. 2, compared with EKF estimated $\Re[\hat{X}_t]$. From both plots, with $\text{SNR} = 0.1$, the signal is submerged in large noise. However, the EC estimated signal (blue) is closer to the synthetic signal (yellow) compared with EKF estimated signal (red). When frequency experiences small wandering in scenario (iii), as displayed in Fig. 2, by estimating the product X_{mn} , we can still extract \hat{X}_t with higher accuracy than EKF estimated signal.

4.3 Detection performance

To quantify the performance of the approximate EC detector, receiver operating characteristic (ROC) curves with different SNRs under scenario (ii) with $q_\Theta = 10^{-1}$ and $w_0 = 0.012$ Hz are displayed in Fig. 3, compared with the EKF detector as well. In Fig. 4, ROCs of the EC and EKF detector under scenario (iii) with $q_\Theta = 10^{-1}$, $q_w = 10^{-8}$ and $w_0 = 0.012$ Hz are plotted. From Fig. 3, as

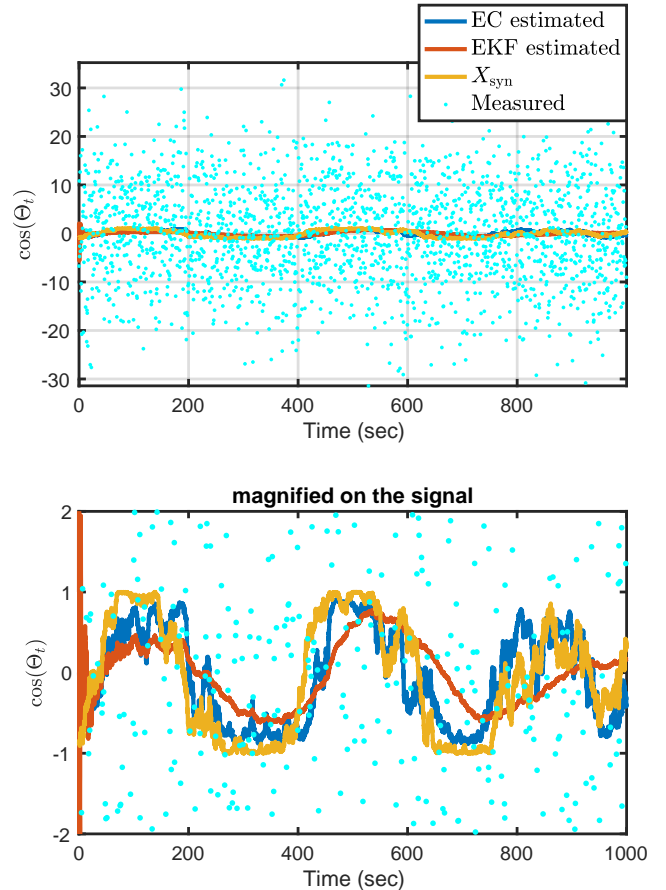


Fig. 1. Conditional mean estimate under scenario (ii): Plot of $\Re[\hat{X}_t]$ estimated by EC (blue) and EKF (red) at $\text{SNR} = 0.1$ with Θ_t defined in (5), where $w_0 = 0.012$ Hz and $q_\Theta = 10^{-2}$. The bottom panel is a magnified version of the top.

SNR drops from 0.1 (top) to 0.0816 (middle) and then to 0.0577 (bottom), Pd of the EC detector (blue) descends from 0.9 to 0.6, then to 0.4 at $\text{Pf} = 10^{-2}$. Fig. 4 exhibits a similar trend, with higher Pd as SNR gets larger. Comparing two top panels between Fig. 3 and Fig. 4, when the frequency is slowly wandering, with $q_w = 10^{-8}$ in Fig. 4, EC experiences a slight degradation, with Pd drops from 0.9 to 0.8 at $\text{SNR} = 0.1$ and $\text{Pf} = 10^{-2}$. Throughout all six panels, the EC detector advantages over the EKF detector with higher Pd across the Pf range, especially when $\text{Pf} < 10^{-2}$.

5. CONCLUSION

In this paper, we focus on estimating and detecting random processes on the circle. The structure of the Neyman-Pearson (or EC) detector is split into two parts: a conditional mean estimate and a log-likelihood ratio detector. The conditional mean estimate, which is described by the nonlinear Kushner stochastic partial differential equation is approximated by filtering the first N moments of the circle-valued signal. Instead of approximating the conditional density of the phase, we characterize the conditional density of the circle-valued signal directly, by pairing it with the moments of the signal. When the frequency is also a random process, in addition to filtering the moment

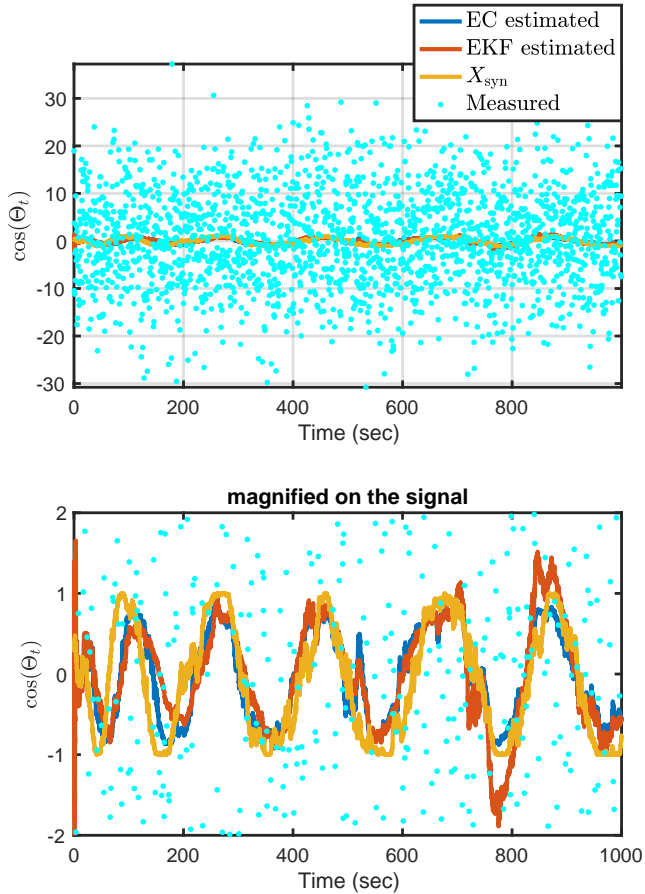


Fig. 2. Conditional mean estimate under scenario (iii): Plot of $\Re[\hat{X}_t]$ estimated by EC (blue) and EKF (red) at SNR = 0.1 with Θ_t defined in (6), where $w_0 = 0.032\text{Hz}$, $q_\Theta = 10^{-2}$ and $q_w = 10^{-8}$. The bottom panel is a magnified version of the top.

function of the signal, we estimate the product of moment functions for frequency and signal, resulting in a deterministic generator.

We perform Monte Carlo simulations to verify the estimation performance by displaying realizations of the EC and EKF estimated signals and plotting the ROC curves for the detection, comparing also with the EKF detector. Overall, EC estimated signal has better tracking (estimating) capacity and higher detection probability than EKF based methods.

ACKNOWLEDGEMENTS

The authors acknowledge support from the Australian Research Council (ARC) through the Centre of Excellence for Gravitational Wave Discovery (OzGrav) (grant number CE170100004) and an ARC Discovery Project (grant number DP170103625).

REFERENCES

Condat, L. (2021). Tikhonov regularization of circle-valued signals. doi:10.48550/ARXIV.2108.02602. URL <https://arxiv.org/abs/2108.02602>.
 Coote, P., Trumpf, J., Mahony, R., and Willems, J.C. (2009). Near-optimal deterministic filtering on the

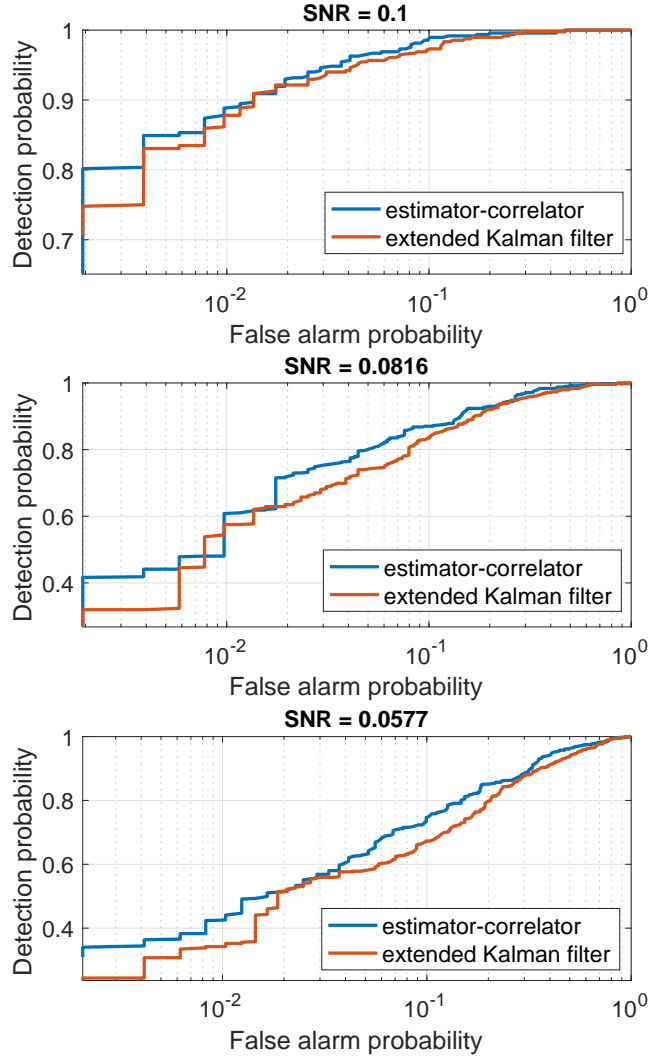


Fig. 3. ROC curves under scenario (ii): false alarm probability vs detection probability as SNR drops from 0.1 (top) to 0.0816 (middle) then to 0.0577 (bottom), with $q_\Theta = 10^{-1}$ and $w_0 = 0.012\text{Hz}$.

unit circle. In *Proceedings of the 48th IEEE Conference on Decision and Control (CDC) held jointly with 2009 28th Chinese Control Conference*, 5490–5495. doi: 10.1109/CDC.2009.5399999.
 Foschini, G.J., Greenstein, L.J., and Vannucci, G. (1988). Noncoherent detection of coherent lightwave signals corrupted by phase noise. *IEEE Transactions on Communications*, 36(3), 306–314.
 Georgiades, C.N. and Snyder, D.L. (1985). A proposed receiver structure for optical communication systems that employ heterodyne detection and a semiconductor laser as a local oscillator. *IEEE Trans. Commun.*, 33(4), 382–384. doi:10.1109/TCOM.1985.1096303. URL <https://doi.org/10.1109/TCOM.1985.1096303>.
 Kailath, T. and Poor, H.V. (1998). Detection of stochastic processes. *IEEE Transactions on Information Theory*, 44(6), 2230–2231.
 Kushner, H. (1967). Nonlinear filtering: The exact dynamical equations satisfied by the conditional mode. *IEEE Transactions on Automatic Control*, 12(3), 262–267.
 Melatos, A., Clearwater, P., Suvorova, S., Sun, L., Moran, W., and Evans, R.J. (2021). Hidden markov

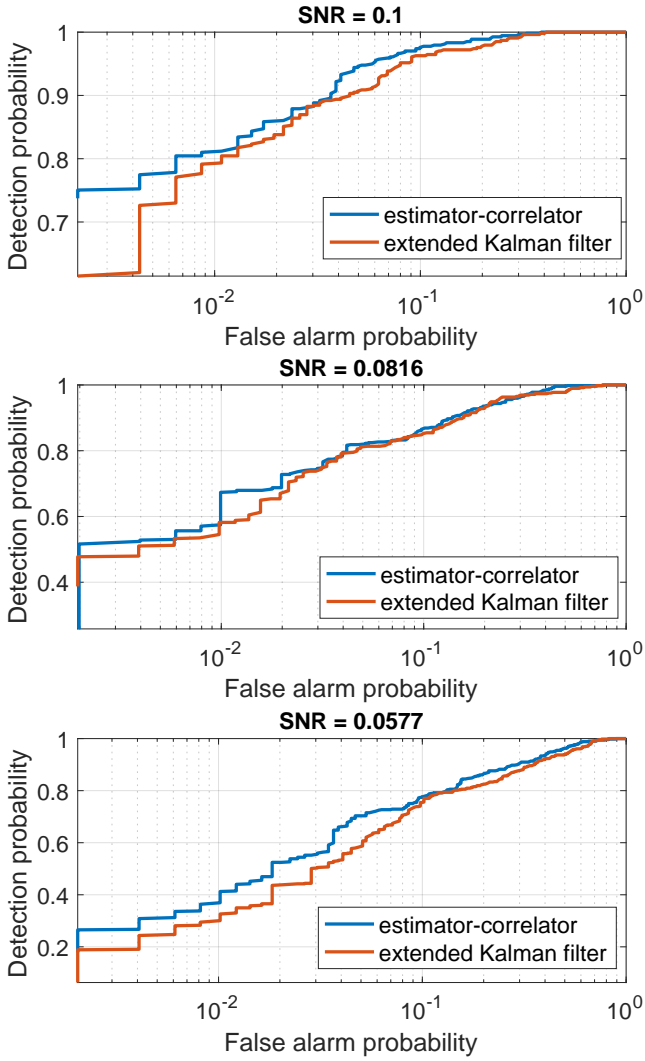


Fig. 4. ROC curves under scenario (iii): false alarm probability vs detection probability as SNR drops from 0.1 (top) to 0.0816 (middle) then to 0.0577 (bottom), with $q_{\Theta} = 10^{-1}$, $q_w = 10^{-8}$ and $w_0 = 0.012\text{Hz}$.

model tracking of continuous gravitational waves from a binary neutron star with wandering spin. iii. rotational phase tracking. *Phys. Rev. D*, 104, 042003. doi:10.1103/PhysRevD.104.042003. URL <https://link.aps.org/doi/10.1103/PhysRevD.104.042003>.

Rusch, L.A. and Poor, H.V. (1995). Effects of laser phase drift on coherent optical cdma. *IEEE journal on selected areas in communications*, 13(3), 577–591.

Scharf, L., Cox, D., and Masreliez, C. (1980). Modulo- 2π phase sequence estimation (corresp.). *IEEE Transactions on Information Theory*, 26(5), 615–620. doi:10.1109/TIT.1980.1056241.

Snyder, D. (1968). The state-variable approach to analog communication theory. *IEEE Transactions on Information Theory*, 14(1), 94–104. doi:10.1109/TIT.1968.1054093.

Suvorova, S., Howard, S.D., and Moran, B. (2021). Tracking rotations using maximum entropy distributions. *IEEE Transactions on Aerospace and Electronic Systems*, 57(5), 2953–2968. doi:10.1109/TAES.2021.3067614.

Suvorova, S., Melatos, A., Evans, R.J., Moran, W., Clearwater, P., and Sun, L. (2018). Phase-continuous frequency line track-before-detect of a tone with slow frequency variation. *IEEE Transactions on Signal Processing*, 66(24), 6434–6442. doi:10.1109/TSP.2018.2877176.

Tam, P. and Moore, J. (1977). A gaussian sum approach to phase and frequency estimation. *IEEE Transactions on Communications*, 25(9), 935–942. doi:10.1109/TCOM.1977.1093926.

Tretter, S. (1985). Estimating the frequency of a noisy sinusoid by linear regression (corresp.). *IEEE Transactions on Information Theory*, 31(6), 832–835. doi:10.1109/TIT.1985.1057115.

Veeravalli, V.V. and Poor, H.V. (1991). Quadratic detection of signals with drifting phase. *The Journal of the Acoustical Society of America*, 89(2), 811–819.

Willsky, A. (1974). Fourier series and estimation on the circle with applications to synchronous communication—i: Analysis. *IEEE Transactions on Information Theory*, 20(5), 577–583. doi:10.1109/TIT.1974.1055280.

Zamani, M., Trumpf, J., and Mahony, R. (2011). Minimum-energy filtering on the unit circle.